Anomalous broad dielectric relaxation in $Bi_{1.5}Zn_{1.0}Nb_{1.5}O_7$ pyrochlore

Stanislav Kamba,* Viktor Porokhonskyy, Alexej Pashkin, Viktor Bovtun, and Jan Petzelt
Institute of Physics, Academy of Sciences of the Czech Republic, Na Slovance 2, 18221 Prague 8, Czech Republic

Juan C. Nino, Susan Trolier-McKinstry, Michael T. Lanagan, and Clive A. Randall
Center for Dielectric Studies, Materials Research Institute, Pennsylvania State University, University Park, Pennsylvania 16802

(Received 18 December 2001; revised manuscript received 6 March 2002; published 19 August 2002)

The complex dielectric response of $Bi_{1.5}Zn_{1.0}Nb_{1.5}O_7$ cubic pyrochlore ceramics was investigated between 100 Hz and 100 THz by a combination of low-frequency capacitance bridges, a high-frequency coaxial technique, time domain transmission THz spectroscopy, and infrared spectroscopy. The data obtained between 10 K and 400 K revealed glasslike dielectric behavior: dielectric relaxation is observed over a wide frequency and temperature range, and the dielectric permittivity and loss maxima shift to higher temperature values by almost 200 K with increasing measuring frequency. The distribution of relaxation frequencies broadens on cooling and can be described by a uniform distribution. The high-frequency end of the distribution at $\sim 10^{11}$ Hz is almost temperature independent and its low-frequency end obeys the Arrhenius Law with an activation energy of ~ 0.2 eV. The relaxation is assigned to the local hopping of atoms in the A and O' positions of the pyrochlore structure among several local potential minima. The barrier height for hopping is distributed between 0 and 0.2 eV. Such an anomalously broad distribution may have its origin in the inhomogeneous distribution of Zn^{2+} atoms and vacancies on Bi^{3+} sites, which gives rise to random fields and nonperiodic interatomic potential. Frequency independent dielectric losses ($1/f$ noise) are observed at low temperatures, which seems to be a universal behavior of disordered systems at low temperatures.

DOI: 10.1103/PhysRevB.66.054106 PACS number(s): 77.22.−d, 78.30.−j, 63.20.−e

I. INTRODUCTION

Appearance of dielectric dispersion below the optical phonon frequency range (neglecting piezoelectric resonances in piezoelectric materials) is a signature of some disorder in the dielectric material. Broadband dielectric spectroscopy, which can be now conducted over a range of 10^{-5}–10^{14} Hz, is a very sensitive and powerful tool for studying the nature of the disorder. This approach is now widely used for studying highly disordered solids like classical glasses[1] and polymers,[2–4] as well as partially disordered solids like dipolar (quadrupolar, orientational, protonic) glasses[6] and relaxor ferroelectrics,[7,8] where the main lattice periodicity is preserved, and only some of the sublattices exhibit disorder. In many systems the dielectric spectra reveal relaxations which slow down on cooling.[2,3] This is a manifestation of local motion of ions with an amplitude substantially larger than that of polar lattice vibrations, but still smaller than interatomic distances. The slowing down indicates that the motion requires a thermally activated hopping over some potential barrier. Assuming that the barrier is uniform for all the charges, the charges hop independently of each other, and the barrier height is temperature independent, the characteristic relaxation frequency f_r (peak in the dielectric loss spectra) should obey the Arrhenius Law,[2,3]

$$f_r = f_\infty \exp\left(\frac{-E_a}{kT}\right), \tag{1}$$

where f_∞ is the relaxation frequency at infinite temperature and E_a is the activation energy, i.e., the barrier height, k is the Boltzmann constant, and T is temperature. In the case of mutually correlated hopping motion, the relaxation frequency usually approximately obeys the Vogel–Fulcher Law,[5,6]

$$f_r = f_\infty \exp\left(\frac{-E_a}{k(T-T_{VF})}\right) \tag{2}$$

for $T > T_{VF}$, where the Vogel–Fulcher temperature T_{VF} describes the finite freezing temperature of the relaxation and the activation energy E_a has the usual meaning only for $T \gg T_{VF}$. At lower temperatures $T \gtrsim T_{VF}$ the activation energy for thermally activated hopping increases and for $T = T_{VF}$ it should diverge, which cannot be, however, experimentally verified down to T_{VF} since near T_{VF} the ergodicity becomes broken.

Disorder, however, inevitably produces random electric fields which introduce some statistical distribution into the local potential barrier heights for charge hopping. Thus, the activation energy should no longer be the same for all hopping ions. This broadens the relaxation in the dielectric spectra and the loss peak compared to the case of a single Debye relaxation. If the distribution is temperature independent (due to frozen random fields) than the broadening becomes exponentially wider on cooling. This is qualitatively observed in many dynamically disordered dielectric systems,[6] but is so far very little investigated experimentally, because it requires an extremely broad frequency range of investigations at cryogenic temperatures.

In this paper we present and describe the broadband dielectric spectra of another type of partially disordered dielectric material, namely $Bi_{1.5}Zn_{1.0}Nb_{1.5}O_7$ with a cubic pyrochlore structure. This material is neither a dipolar glass nor a relaxor ferroelectric. It will be shown that nevertheless the

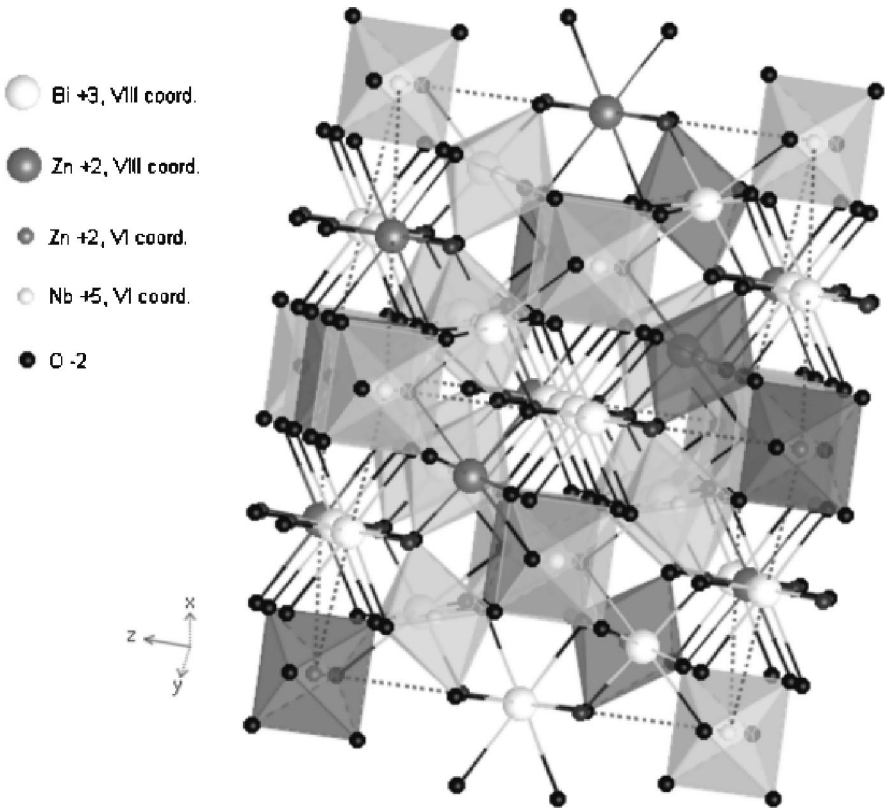

FIG. 1. Crystal structure of cubic $Bi_{1.5}Zn_{1.0}Nb_{1.5}O_7$. 21% of Bi atoms arranged along $\langle 1\bar{1}0\rangle$ directions are substituted by Zn atoms, 4% of A sites are vacant. Each atom on the A site is actually disordered among 6 equivalent positions, O' atoms are disordered among 12 equivalent sites (Ref. 19). 25% of Nb atoms are substituted by Zn atoms.

dielectric spectra reveal some features which are common with other disordered systems so far studied.

Bi pyrochlore ceramics were discovered in the early 1970s[9,10] and have attracted additional study during the last 5 years due to their possible applications in high frequency capacitors and microwave resonators. The permittivity ε' is relatively large (80–180),[11–14] the dielectric losses are small ($\tan\delta \sim 10^{-3}$ in the kHz range),[13–15] and it is possible to prepare ceramics with temperature coefficients of permittivity, TCε, smaller than 10 ppm/ °C.[16] Very important for an application in integrated circuits is the fact that the permittivity of Bi-pyrochlore thin films is not effected by thickness[17] and also that low crystallization temperatures ($\sim$550 °C) can be achieved.[17,18] There are two main phases in the Bi_2O_3–ZnO–Nb_2O_5 system: $Bi_{1.5}Zn_{1.0}Nb_{1.5}O_7$, in which at least some Zn atoms occupy A site positions,[19] with $\varepsilon' \sim 160$ at room temperature and the cubic pyrochlore structure (space group $Fd\bar{3}m$-O_h^7, $Z=8$, see Fig. 1)[13,19,20] and $Bi_2(Zn_{1/3}Nb_{2/3})_2O_7$ which has $\varepsilon' \sim 80$ and a pyrochlore-related crystal structure that is often reported as pseudo-orthorhombic,[13] but is actually monoclinic.[21,22] Both compounds can be generally written as $(Bi_{3x}Zn_{2-3x})(Zn_xNb_{2-x})O_7$ with $x=0.5$ (cubic) and $x=2/3$ (monoclinic), respectively. The temperature coefficient of capacitance is negative for cubic $Bi_{1.5}Zn_{1.0}Nb_{1.5}O_7$ (TCε $=-400$ ppm/ °C), while monoclinic $Bi_2(Zn_{1/3}Nb_{2/3})_2O_7$ has a positive TC$\varepsilon=150$ ppm/ °C.[13] Two-phase samples with appropriate compositions achieve TCε close to zero with $\varepsilon' \approx 100$ and $tan\delta < 10^{-2}$.[16]

The $A_2B_2O_7$ pyrochlore structure is often described by the formula $B_2O_6 \cdot A_2O'$, which emphasizes that the structure is built of two interpenetrating networks: BO_6 octahedra sharing vertices form a three-dimensional network (see Fig. 1) resulting in large cavities which contain the O' and A atoms in an A_2O' tetrahedral net.[19] A-cations are randomly displaced by $\sim$0.39 Å from the ideal eightfold coordinated positions. The displacement occur along the six $\langle 112\rangle$ directions perpendicular to the O'–A–O' links. In addition, the O' ions are randomly displaced by $\sim$0.46 Å along all twelve $\langle 110\rangle$ directions.[23]

The effect of various chemical substitutions on the structure and dielectric properties of Bi-based pyrochlores was investigated by several authors.[15,23–26] An attempt to minimize TCε in $Bi_{1.5}Zn_{1.0}Nb_{1.5}O_7$ by doping with Bi_3NBO_7 (TC$\varepsilon=+170$ ppm/ °C, $\varepsilon'=100$) was published in Ref. 27. The resulting pyrochlore-fluorite two-phase samples exhibit TCε between 80 and 200 ppm/ °C and ε' varies between 80 and 100, depending on the concentration of Bi_3NbO_7.

Dielectric measurements between 2 kHz and 1 MHz revealed broad dielectric relaxation in cubic $Bi_{1.5}Zn_{1.0}Nb_{1.5}O_7$ bulk ceramics[14] and thin films[17] at cryogenic temperatures. The dielectric permittivity is also tunable with an electric field, while the dielectric loss remains field independent.[17] Hysteresis loop measurements revealed no polar order at 4.2 K after cooling a thin film under a bias field of 830 kV/cm.[17] The aim of this paper is the extension of the dielectric study to higher frequencies (up to 100 THz) to understand better the dielectric dispersion mechanism.

II. EXPERIMENTAL PROCEDURE

$Bi_{1.5}Zn_{1.0}Nb_{1.5}O_7$ ceramics were prepared by conventional powder processing techniques; a detailed description

can be found elsewhere.[28] The relative density of the obtained ceramics was higher than 96%.

The low-frequency dielectric response in the range of 100 Hz–1 MHz was measured using a HP 4284 LCR meter with an ac field of 1 V/mm on 3-mm-diam sintered disks. An APD Cryogenics cryostat system (Model HC-2) was used for measurements down to 12 K.

Dielectric measurements in the high-frequency (HF) range of 1 MHz–1.8 GHz were performed using a computer controlled HF dielectric spectrometer equipped with an HP 4291B Impedance Analyzer, a NOVOCONTROL BDS 2100 coaxial sample cell and a SIGMA SYSTEM M18 temperature chamber (operation range 100–570 K). The impedance of a cylindrical sample (diameter 1.5 mm, height 3.5 mm) with Au electrodes sputtered on the cylinder ends was recorded on cooling at a rate of 1 K/min. The dielectric parameters were calculated taking into account the electromagnetic field distribution in the sample.[29,30]

A custom made time-domain terahertz transmission spectrometer was used to obtain the complex dielectric response in the range from 3 cm^{-1} to 30 cm^{-1} (90–900 GHz). The technique itself is suitable up to 80 cm^{-1}, but above 30 cm^{-1} the samples were opaque. This spectrometer uses a femtosecond Ti:sapphire laser and a biased large-aperture antenna from a low-temperature grown GaAs as a THz emitter, and an electro-optic sampling detection technique. This measuring technique is described in detail elsewhere.[31] A polished plane-parallel 100 μm thick disk with a diameter of 6 mm was studied. An Optistat CF cryostat with mylar windows (with thicknesses of 25 and 50 μm for the inner and outer windows, respectively) was used for measurements down to 10 K.

Room temperature infrared reflectivity spectra were obtained using a Fourier transform spectrometer (Bruker IFS 113v) in the frequency range of 20–3300 cm^{-1} (0.6–100 THz). Low-temperature measurements down to 10 K were performed up to 650 cm^{-1} only because the polyethylene windows used in the Optistat CF cryostat (Oxford Ins.) are opaque at higher frequencies. Pyroelectric deuterated triglycine sulfate detectors were used for the room temperature measurement, while a highly sensitive, helium cooled (1.5 K) Si bolometer was used for the low-temperature measurements. A disk-shaped sample with a diameter of 9 mm and thickness of 2 mm was investigated. A micro-Raman spectrum was excited with the 514.5 nm line of an Ar laser and recorded in the back scattering geometry using a Renishaw Ramascope at room temperature. The low-frequency cutoff $\sim$60 cm^{-1} is determined by the notch filter which removes the strong elastically scattered light signal from the spectrum.

III. RESULTS AND DISCUSSION

The temperature dependence of the real and imaginary parts of dielectric function for $Bi_{1.5}Zn_{1.0}Nb_{1.5}O_7$ at selected frequencies between 1 kHz and 1 GHz and calculated from the THz data at 300 GHz is shown in Fig. 2. The data in the range below 100 kHz were already published in Ref. 14; the values were multiplied by 1.14 to match the HF permittivity.

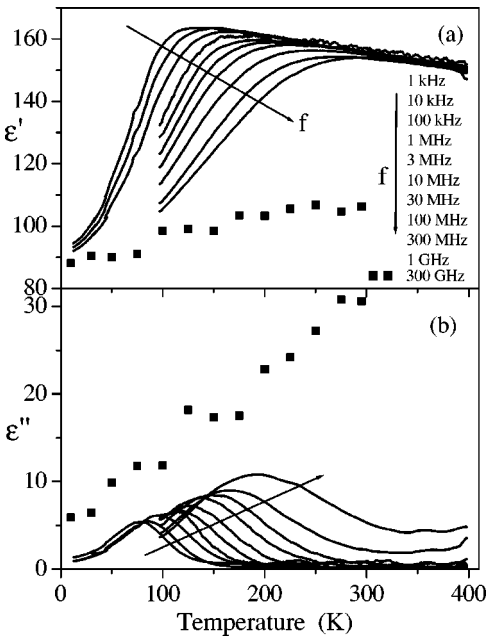

FIG. 2. Temperature dependence of the real (a) and imaginary (b) part of dielectric permittivity at selected frequencies between 1 kHz and 300 GHz (full squares).

This small difference is probably a function of minor differences in the measurement approaches. The HF data were used as reference because they are very accurate at room temperature, where calibration of the spectrometer was done.

Infrared reflectivity spectra at 10 and 300 K are shown in Fig. 3. The spectral range above 1000 cm^{-1} is not shown because the reflectivity is flat at frequencies approaching the value given by the high-frequency permittivity ε_∞. The lack of distinct changes between 300 K and 10 K implies that no structural phase transition occurs on cooling. The complex dielectric response $\varepsilon^*(\omega)$ in the infrared range can be obtained from the reflectivity $R(\omega)$ via

$$R(\omega)=\left|\frac{\sqrt{\varepsilon^*(\omega)}-1}{\sqrt{\varepsilon^*(\omega)}+1}\right|^2, \tag{3}$$

where $\varepsilon^*(\omega)=\varepsilon'(\omega)-j\varepsilon''(\omega)$ was treated using the sum of several damped oscillators plus high frequency permittivity ε_∞ originating from the electronic polarization,

$$\varepsilon^*(\omega)=\varepsilon^*_{\mathrm{ph}}(\omega)+\varepsilon_\infty=\sum_{i=1}^{n}\frac{\Delta\varepsilon_i\omega_i^2}{\omega_i^2-\omega^2+j\omega\gamma_i}+\varepsilon_\infty. \tag{4}$$

ω_i, γ_i, and $\Delta\varepsilon_i$ denote the eigenfrequencies, dampings, and contribution to the static permittivity from the jth polar phonon mode, respectively, and $\varepsilon^*_{\mathrm{ph}}(\omega)$ is the complex phonon permittivity.

The unpolarized micro-Raman spectrum of a $Bi_{1.5}Zn_{1.0}Nb_{1.5}O_7$ ceramic taken at room temperature is shown in Fig. 4. The experimental spectrum $I(\omega)$ was fitted with the sum of several Gaussian curves $I(\omega)=\Sigma I_{0i}\exp\{-[(\omega-\omega_i)/\gamma_i]^2\}+\mathrm{const}$, as shown in Fig. 4. The parameters of the modes seen in the infrared and Raman

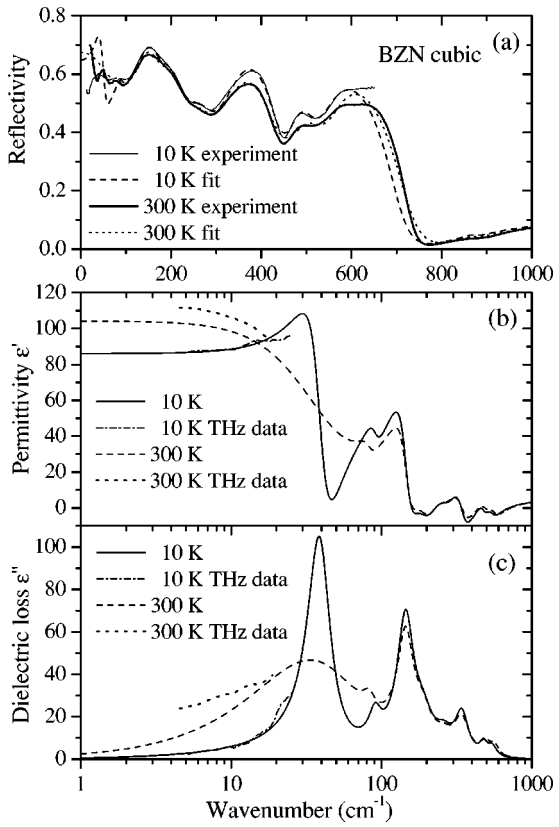

FIG. 3. Infrared reflectivities (a) at 10 and 300 K together with the real (b) and imaginary (c) parts of permittivity calculated from the fits to the reflectivities and submillimeter data with Eqs. (3) and (4).

spectra are summarized in Table I. Note the unusually large damping of most modes. This is consistent with the highly disordered structure of $Bi_{1.5}Zn_{1.0}Nb_{1.5}O_7$

It is interesting to compare the number of phonon modes observed in infrared and Raman spectra with the number of permitted modes using factor-group analysis. According to a very recent structural refinement of cubic $Bi_{1.5}Zn_{0.92}Nb_{1.5}O_{6.92}$, the atoms in A sites occupy one of 6 closely spaced possible positions and each O' atom is disordered among 12 positions.[19] In this case the factor group analysis of cubic $Bi_{1.5}Zn_{1.0}Nb_{1.5}O_7$ yields the following phonon modes in the center of the Brillouin zone (assuming some occupancy of all the sites simultaneously, which gives the upper estimate of the expected modes number[32])

$$\Gamma = 2A_{1u} + 6A_{2u} + 2A_{2g} + 8E_u + 5A_{1g}(R) + 7E_g(R) + 13F_{2g}(R) + 15F_{1u}(IR) + 11F_{2u} + 10F_{1g} \quad (5)$$

including one F_{1u} acoustic triplet. This means that 14 F_{1u} modes are infrared active, 25 modes (of symmetries A_{1g}, E_g, and F_{2g}) should be Raman active and the rest of the modes are silent (i.e., inactive). If the atoms in A and O' sites were not disordered but ordered in the central sites as was assumed in an earlier Ref. 20, the factor group analysis yields

$$\Gamma = 3A_{2u} + 3E_u + A_{1g}(R) + E_g(R) + 4F_{2g}(R) + 8F_{1u}(IR) + 4F_{2u} + 2F_{1g} \quad (6)$$

so that only 7 infrared and 6 Raman active modes are allowed in the spectra. In our case 9 and 8 modes were needed to fit the infrared reflectivity and Raman spectra, respectively, which supports the structure refinement with disorder.

The high damping of the lowest frequency phonon seen in the infrared and THz spectra at ~ 50 cm^{-1} also supports the disorder on the A sites. This mode, assigned in Refs. 23,33 as the 0'-Bi-0' bending vibration is overdamped (see Fig. 3). Our preliminary THz and infrared data revealed that the lowest-frequency phonon mode is underdamped in monoclinic $Bi_2(Zn_{1/3}Nb_{2/3})_2O_7$, where Bi atoms are fully ordered. Radio-frequency permittivity of $Bi_2(Zn_{1/3}Nb_{2/3})_2O_7$ is completely described by phonon contributions and no dielectric relaxation was observed below the polar phonon frequencies.

The fit to the infrared reflectivity data for $Bi_{1.5}Zn_{1.0}Nb_{1.5}O_7$ was combined with the more accurate experimental dielectric data in the range of 3–30 cm^{-1} ob-

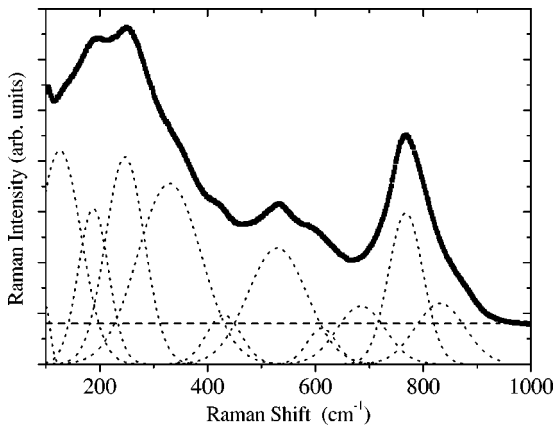

FIG. 4. Room-temperature micro-Raman scattering of $Bi_{1.5}Zn_{1.0}Nb_{1.5}O_7$ ceramics together with the result of Gaussian fit.

TABLE I. Parameters of the observed phonon modes active in infrared and Raman spectra. Frequencies ω_i and dampings γ_i of modes are in cm^{-1}, $\Delta\varepsilon_i$ is dimensionless and the Raman strengths I_{0i} are in arbitrary units.

	IR modes			Raman modes		
No.	ω_i	$\Delta\varepsilon_i$	γ_i	ω_i	I_{0i}	γ_i
1	53.5	67.2	102	100	228	20
2	83.0	1.6	18	126	843	93
3	146.0	15.0	45	188	613	66
4	190	5.8	67	247	817	85
5	259.5	2.2	86	329	712	139
6	344.5	5.0	99	430	194	76
7	490.5	1.2	99	529	458	129
8	565.0	0.9	95	612	142	64
9	872.5	0.006	32	685	229	105
10	...	...	...	768	597	76
11	...	...	...	831	240	108

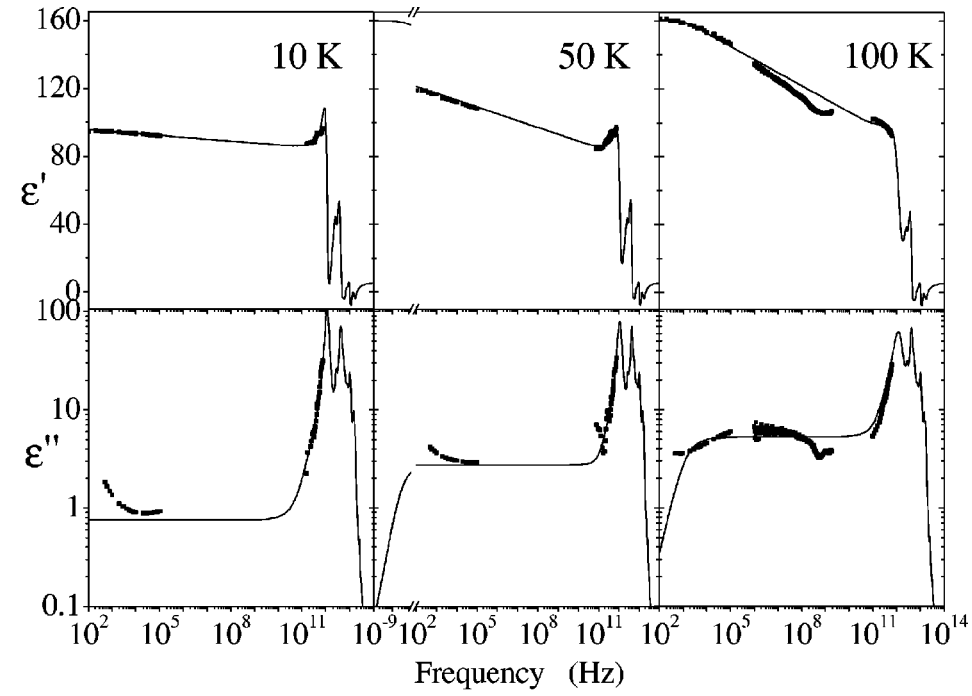

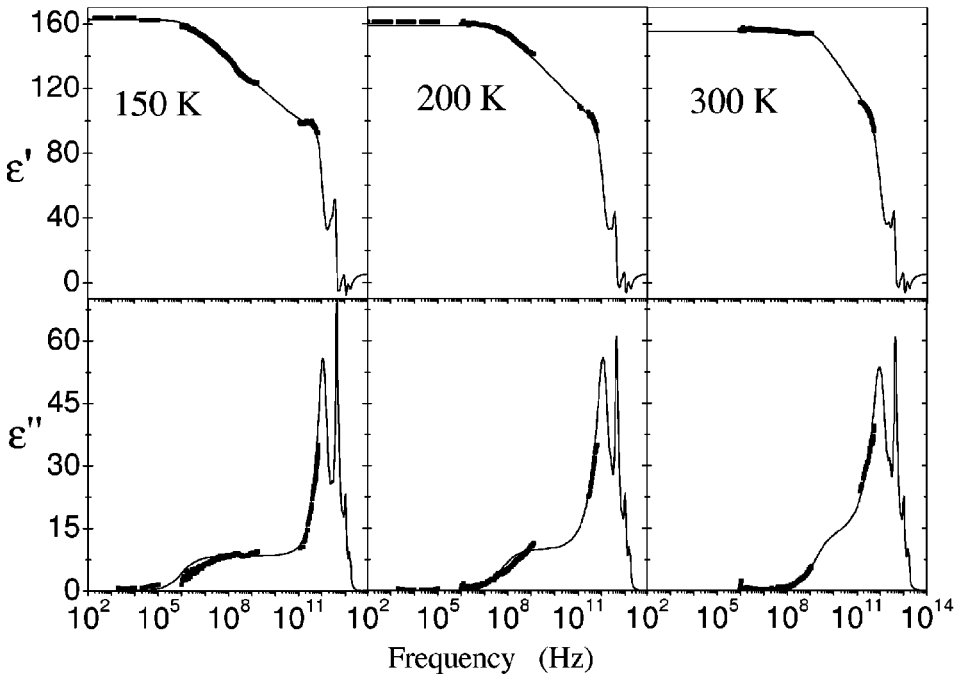

FIG. 5. Frequency dependence of the real and imaginary parts of permittivity at selected temperatures between (a) 10 and 100 K [note the log–log scale for $\varepsilon''(\omega)$] and (b) 150 up to 300 K. Note the frequency scale change at 50 K. The low-frequency increase in $\varepsilon''(\omega)$ below 10^3 Hz at 10 and 50 K is an instrumental effect.

tained from time-domain THz transmission spectroscopy. The oscillator fit was sufficient below 100 K, but Figs. 3(b) and 3(c) show that the oscillator fit is not able to describe the THz data at 300 K. An additional relaxation was required to explain the high submillimeter permittivity and dielectric loss. The permittivity below 2 GHz is higher than the submillimeter permittivity. In addition the dielectric loss observed over the broad spectral region is indicative of a broad dielectric relaxation below phonon frequencies, which is not compatible with a single Debye relaxation. Therefore we attempted to describe the relaxation spectra with a distribution of Debye relaxation frequencies $T(\Omega)$,[34,35]

$$\varepsilon^*(\omega)=\varepsilon_\infty+\varepsilon^*_{\mathrm{ph}}+\int_0^\infty \frac{T(\Omega)}{\Omega+j\omega}\,\mathrm{d}\Omega. \tag{7}$$

For simplicity $T(\Omega)$ was assumed to be a step function,

$$T(\Omega)=\begin{cases}0, & \Omega<f_1 \text{ or } \Omega>f_2\\ g, & f_1<\Omega<f_2.\end{cases} \tag{8}$$

The uniform $T(\Omega)$ corresponds to a constant distribution of equally strong Debye relaxations between some upper (f_2) and lower (f_1) frequencies. In real materials, the shape of $T(\Omega)$ is probably smooth rather than steplike, but this was

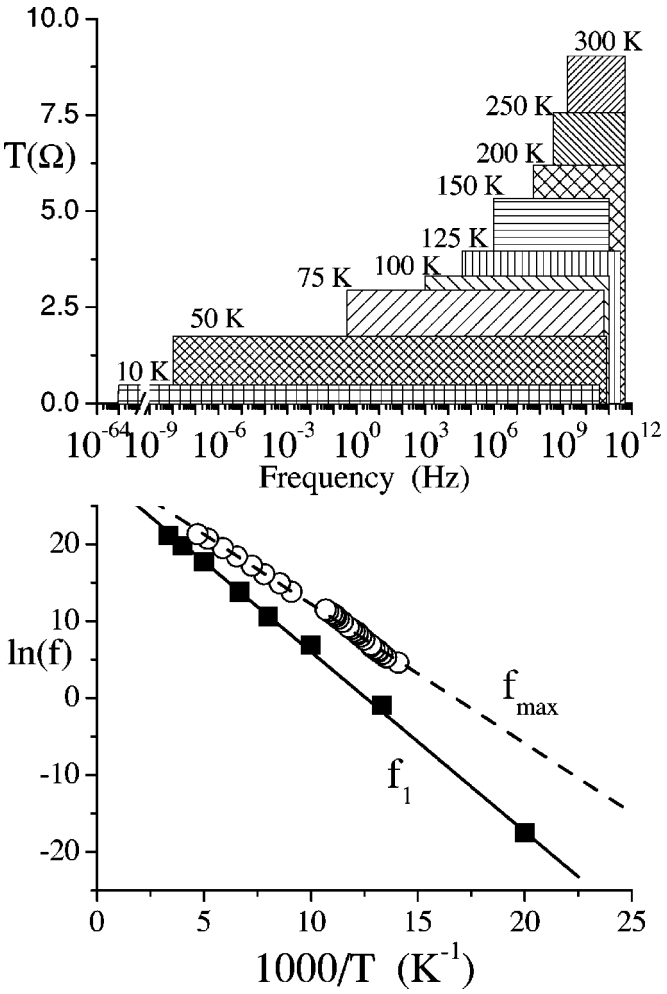

FIG. 6. (a) Distribution function T(Ω) of Debye relaxation frequencies at selected temperatures. (b) The Arrhenius plot of f_1 (shown as full squares, $f_\infty = 6.129 \cdot 10^{12}$ Hz, $E_a = 0.202$ eV) together with the Arrhenius plot of frequencies $f_{\max}$ corresponding to the ε''(T) maxima at fixed frequencies (see open circles, $f_\infty = 1.502 \cdot 10^{13}$ Hz, $E_a = 0.156$ eV).

not considered here in a first approximation. $T(\Omega)$ is normalized by the total dielectric strength of the relaxation,

$$\Delta\varepsilon_R = \varepsilon_0 - \varepsilon_\infty - \sum_{i=1}^{n} \Delta\varepsilon_i = \int_0^\infty \frac{T(\Omega)}{\Omega}\, d\Omega = g \ln\frac{f_2}{f_1}. \quad (9)$$

This model is a simple one, but it allows us to estimate the width, and the upper and lower limits of the relaxation frequency distribution. Such a uniform $T(\Omega)$ was also used for analysis of dipolar glass $Rb_{1-x}(NH_4)_xH_2PO_4$ (Ref. 36) and the relaxor ferroelectrics $PbMg_{1/3}Nb_{2/3}O_3$ and $Pb_{1-x}La_xZr_{1-y}Ti_yO_3$ (PLZT).[37,38] The integral in Eq. (7) with a uniform $T(\Omega)$ can be transformed into the following expression:

$$\varepsilon^*(\omega) = \varepsilon_\infty + \varepsilon^*_{\rm ph} + \frac{g}{2}\ln\left(\frac{f_2^2+\omega^2}{f_1^2+\omega^2}\right) - jg\left[\arctan\left(\frac{f_2}{\omega}\right) - \arctan\left(\frac{f_1}{\omega}\right)\right]. \quad (10)$$

Figure 5 shows the frequency dependencies of the real and imaginary parts of the dielectric functions at selected temperatures in the frequency range of 100 Hz–100 THz. In this figure, the experimental data from low- and high-frequency dielectric measurements were combined with submillimeter and infrared data. The solid lines show the results of the fits with Eqs. (4) and (10). A good agreement between the theoretical curves and experimental data is seen. Experimental ε' values at 100 K are lower than the fit probably because the accuracy of the HF spectrometer becomes lower as the operation temperature decreases from room temperature, where calibration of coaxial measuring cell was performed. Small discrepancies in ε'' at frequencies in the vicinity of f_1 are presumably due to the fact that the real distribution function $T(\Omega)$ does not undergo steplike changes, but is actually smooth. The fits at low temperatures were performed under the assumption that the static permittivity, $\varepsilon_0 = 160$, is temperature independent as usually assumed for dipolar glasses.[45] In fact from theoretical considerations for a system of independent dipoles, ε_0 should increase with decreasing temperature according to the Curie Law,

$$\varepsilon_0(T) = \frac{C}{T} + \text{const}, \quad (11)$$

but the fit to $\varepsilon_0(T)$ with this dependence yields such a small Curie constant ($C < 2500$ K) that the temperature dependence of ε_0 is down to 50 K negligible.

The distribution functions of the relaxation frequencies, $T(\Omega)$, obtained from the fits of the dielectric dispersion are shown in Fig. 6(a). It shows that the high-frequency limit f_2 of $T(\Omega)$ is almost temperature independent (within the experimental accuracy), and reaches values between 100 GHz and 1 THz, which is close to optical phonon frequencies. f_1—the low-frequency edge of $T(\Omega)$—moves from the GHz range at 300 K down to the Hz range at 75 K, and then rapidly to the sub-Hz range on further cooling. At 10 K, the fit yields an f_1 of 10^{-63} Hz, on the assumption of a constant static permittivity and even less for the case of increasing static permittivity. This means that ε' will never reach the static value in real time and ε'' should be nonzero and frequency independent practically at all frequencies below 100 GHz.

Our results show that the Arrhenius Law [Eq. (1)] satisfactorily describes the temperature behavior of f_1. The Arrhenius plot of $\ln f_1(1000/T)$ is shown in Fig. 6(b) by solid squares; the parameters of the fit ($f_\infty = 6.13 \times 10^{12}$ Hz, $E_a = 0.202$ eV or $E_a/k = 2345$ K) are reasonable. The activation energy E_a characterizes the highest potential barrier and f_1 consequently corresponds to the frequency of the slowest group of hopping ions.[36] On the other hand, the essentially temperature independent f_2 means that the barrier heights distribution is spread down to zero. When f_1 data were refitted using the more general Vogel–Fulcher Law [Eq. (2)] the resulting freezing temperature $T_{\rm VF}$ was only 0.4 K, which supports the simpler Arrhenius fit. When the temperature dependence of dielectric loss maxima [from Fig. 2(b)] were fitted, again Arrhenius behavior was obtained with $f_\infty = 1.50 \times 10^{13}$ Hz and $E_a = 0.156$ eV (see open points in Fig. 6). One can see that the difference between the two temperature dependencies is quite pronounced. Let us note that the fit using frequency spectra has a clear physical meaning associ-

ated with slowing down of some dissipative process, whereas the meaning of fit to the maxima in temperature dependencies of loss (or permittivity) at several fixed frequencies though widely used is much less physically transparent especially in case of polydispersive relaxation and/or strong temperature dependence of the dielectric strength. However, there is a trend to use the latter fitting procedure, since it is experimentally more easily achieved with a narrower frequency range of measurements.

Let us discuss the origin of the relaxation. The structure refinement in Ref. 19 suggests that the cubic pyrochlore structure can tolerate considerable Zn substitution on the A site. In our sample 21% of Bi^{3+} atoms are replaced with Zn^{2+} atoms (note the different valence of the atoms) and 4% of the A positions remain vacant [i.e., the proper chemical formula of the cubic pyrochlore phase is $(Bi_{1.5}Zn_{0.42})(Zn_{0.5}Nb_{1.5})O_{6.92}$].[19] Each A atom occupies one of 6 closely spaced possible positions, each O' atom is disordered among 12 positions. The relaxation might stem from the hopping of dynamically disordered A and O' atoms among the closely spaced possible positions. Moreover, it is clear that the inhomogeneous distribution of Zn^{2+} atoms and vacancies on the Bi^{3+} sites gives rise to additional random fields. This could yield multiwell potentials that have a wide distribution of heights, and therefore transition rates, for Bi^{3+} and Zn^{2+} cations. Such an interatomic potential can cause a broad dielectric relaxation. Our data show that in fact this distribution goes essentially from 0 (consistent with the temperature independent f_2) to about $E_a \approx 0.2$ eV. As already mentioned, the closely related monoclinic $Bi_2(Zn_{1/3}Nb_{2/3})_2O_7$, which has completely ordered Bi atoms with no Zn substitution on the A sites[22] exhibits no dielectric relaxation below phonon frequencies. On the other hand, in $Bi_{1.5}Zn_{1.0}Ta_{1.5}O_7$, which probably also has disordered Bi and Zn atoms on the A sites, low frequency dielectric relaxation was observed. However, its contribution to the static permittivity $\Delta\varepsilon_R$ was only ~ 10, in comparison to $\sim 60-70$ in the case of $Bi_{1.5}Zn_{1.0}Nb_{1.5}O_7$.[39]

A broad frequency range with nearly constant loss is frequently seen in other disordered systems like conducting ionic glasses, melts and crystals (see Refs. 40,41) as well as in dipolar glass systems [e.g., $Rb_{1-x}(NH_4)_xH_2PO_4$ (Refs. 6,42–45)] and relaxor ferroelectrics[38,46,47] at low temperatures. Frequency independent losses are seen also in polymers and supercooled liquids and are known as the $1/f$ noise.[3,4,48] Also the dielectric response of the relaxor ferroelectric PLZT ceramics can be successfully fitted with a uniform distribution of relaxation frequencies $T(\Omega)$.[38] Since the static permittivities of ferroelectric relaxors and the cubic Bi pyrochlore are substantially higher than in ionic conductors, supercooled liquids and polymers, the value of dielectric loss ε'' is by 2–3 orders of magnitude higher.

It should be noted that the width of the relaxation-time distribution can be determined also from a special model-independent frequency–temperature plot (so called Kutnjak plot)[45] which was successfully applied to $Rb_{1-x}(ND_4)_xD_2PO_4$ and ferroelectric relaxors.[45–47] In all the cases, under the assumption of constant static permittivity at low temperatures, the high-frequency edge of relaxation frequencies was found to follow the Arrhenius Law with a very small activation energy (not much different from our case), whereas the low-frequency edge obeyed the Vogel–Fulcher Law. This indicates some correlation effects between the dipoles which leads to the formation of polar clusters at low temperatures. In our case of $Bi_{1.5}Zn_{1.0}Nb_{1.5}O_7$ the low-frequency edge follows the Arrhenius law which indicates that the hopping of the atoms in the A-positions is mutually independent and no cluster formation is expected.

The physical mechanism that gives rise to the frequency independent loss spectra is not completely understood generally, but it seems that this phenomenon is universal.[40,41] It is highly probable that the origin of constant loss in ferroelectric relaxors, dipolar glasses, supercooled liquids, ionic conductors, and Bi pyrochlore is the same—random fields produce distributions of multiwell potentials with a wide distribution of transition rates for hopping of dynamically disordered ions. Such a picture always yields $1/f$ noise, but only at sufficiently low temperatures. Our point is therefore that constant dielectric loss should also be expected in other disordered systems, but only at low temperatures. This differs from the meaning of other authors studying ionic conducting glasses,[40,41] where the constant loss contribution was evaluated from the medium temperature dielectric spectra by subtracting a contribution of the dc conducting ions dominating at low frequencies. In our opinion, their analysis and conclusion about constant loss contribution are justified only in the higher-frequency range and its low-frequency cutoff as a function of temperature cannot be properly followed. In our case, the data analysis is simpler and more straightforward because the conduction contribution to the dielectric response is negligible at all temperatures. This enabled us to conclude that the low-frequency cut-off of the constant loss mechanism is thermally activated, as follows also from our simple model of broad frozen potential barrier distribution for local hopping of disordered ions.

IV. SUMMARY

The complex dielectric response of $Bi_{1.5}Zn_{1.0}Nb_{1.5}O_7$ between 100 Hz and 100 THz revealed dielectric relaxation below the polar phonon frequencies. Its dielectric strength $\Delta\varepsilon_R \cong 70$ is comparable with the phonon contribution. At room temperature the relaxation occurs at frequencies above 10^8 Hz. On cooling the relaxation anomalously broadens and below 100 K it spreads beyond the lowest measured frequency of 100 Hz. The dielectric loss is nearly frequency independent at low temperatures and the complex dielectric dispersion could be well described by a uniform distribution of relaxation frequencies. The high-frequency limit of relaxation frequencies is nearly temperature independent ($f_2 \approx 10^{11}$ Hz); the low-frequency limit f_1 follows the Arrhenius Law. The relaxation might stem from the hopping of dynamically disordered Bi and Zn atoms at the A sites (each of the A atoms occupy one of 6 equivalent, closely spaced positions) and hopping of O' atoms among 12 sites. The disorder was confirmed by infrared and Raman spectra. The broad distribution of relaxation frequencies has its origin in

the inhomogeneous distribution of Zn^{2+} atoms and vacancies on Bi^{3+} sites which induce random fields. Our data show that the barrier heights distribution for the hopping of the disordered ions reaches from about 0.2 eV essentially to 0 and is temperature independent. A nearly constant dielectric loss has been observed at low temperatures in many dynamically disordered materials. It can be concluded that this effect has always a common origin—random fields produce distributions of multiwell potentials with a wide distribution of transition rates for hopping of some sort of dynamically disordered ions.

ACKNOWLEDGMENTS

The work was supported by the Grant Agency of the Czech Republic (Projects Nos. 202/01/0612, 203/99/0067, and 202/00/1198), Grant Agency of Academy of Sciences (Projects Nos. A1010203 and AVOZ1-010-914), Ministry of Education of the Czech Republic (Project No. COST OC 525.20/00), the Center for Dielectric Studies, Intel, and the Semiconductor Research Corporation. The authors would like to thank J. Pokorný for measurement and fitting of Raman spectrum.

*Electronic address: kamba@fzu. cz

[1] S. Benkhof, T. Blochowicz, A. Kudlik, C. Tschirwitz, and E. Rössler, Ferroelectrics **236**, 193 (2000).
[2] A.K. Jonscher, *Dielectric Relaxation in Solids* (Chelsea Dielectrics Press, London, 1983).
[3] A.K. Jonscher, *Universal Relaxation Law* (Chelsea Dielectrics Press, London, 1996).
[4] J.P. Runt and J.J. Fitzgerald, *Dielectric Spectroscopy of Polymeric Materials* (American Chemical Society, Washington, D.C., 1997).
[5] E. Courtens, Phys. Rev. Lett. **52**, 69 (1984).
[6] U.T. Höchli, K. Knorr, and A. Loidl, Adv. Phys. **39**, 405 (1990).
[7] Z.-G. Ye, Key Eng. Mater. **155-156**, 81 (1998).
[8] G.A. Samara, *Ferroelectricity Revisited: Advances in Materials and Physics*, in *Solid State Physics* (Academic, San Diego, 2001), Vol 56.
[9] G.I. Golovshikova, V.A. Isupov, A.G. Tutov, I.E. Myl'nikova, P.A. Nikitina, and O.I. Tulinova, Sov. Phys. Solid State **14**, 2539 (1973).
[10] V.A. Isupov, Ferroelectr. Rev. **2**, 115 (2000).
[11] D. Liu, Y. Liu, S. Huang, and X. Yao, J. Am. Ceram. Soc. **76**, 2129 (1993).
[12] D.P. Cann, C.A. Randall, and T.R. Shrout, Solid State Commun. **100**, 529 (1996).
[13] X. Wang, H. Wang, and X. Yao, J. Am. Ceram. Soc. **80**, 2745 (1997).
[14] J.C. Nino, M.T. Lanagan, and C.A. Randall, J. Appl. Phys. **89**, 4512 (2001).
[15] H. Wang, D. Zhang, X. Wang, and X. Yao, J. Mater. Res. **14**, 546 (1999).
[16] S. L. Swartz and T. R. Shrout, U.S. Patent No. 5,449,652 (1995).
[17] W. Ren, S. Trolier-McKinstry, C.A. Randall, and T.R. Shrout, J. Appl. Phys. **89**, 767 (2001).
[18] X. Wang, W. Yao, B. Huang, and X. Cai, Chinese Patent No. 1089247A, Nov. 23, 1994.
[19] I. Levin, T. G. Amos, J. C. Nino, T. A. Vanderah, C. A. Randall, and M. T. Lanagan, J. Solid State Chem. (to be published).
[20] G. Jeanne, G. Desgardin, and B. Raveau, Mater. Res. Bull. **9**, 1321 (1974).
[21] H. Wang, X. Wang, and X. Yao, Ferroelectrics **195**, 19 (1997).
[22] I. Levin, T. G. Amos, J. C. Nino, T. A. Vanderah, I. M. Reaney, C. A. Randall, and M. T. Lanagan, J. Mater. Res. **17**, 1406 (2002).
[23] M.A. Subramanian, G. Aravamudan, and G.V. Subba Rao, Prog. Solid State Chem. **15**, 55 (1983).
[24] H. Wang, X. Yao, and F. Xia, Ferroelectrics **229**, 285 (1999).
[25] M. Valant and P.K. Davies, J. Mater. Sci. **34**, 5437 (1999).
[26] M. Valant and P.K. Davies, J. Am. Ceram. Soc. **83**, 147 (2000).
[27] H. Wang and X. Yao, J. Mater. Res. **16**, 83 (2001).
[28] J.C. Nino, M.T. Lanagan, and C.A. Randall, J. Mater. Res. **16**, 1460 (2001).
[29] V. M. Petrov, Dielectric measurements of Ferroelectrics, Moscow, 1972 (in Russian).
[30] J. Grigas, *Microwave Dielectric Spectroscopy of Ferroelectrics and Related Materials* (Gordon and Breach, Amsterdam 1996).
[31] P. Kužel and J. Petzelt, Ferroelectrics **239**, 79 (2000).
[32] I. Hrubá, S. Kamba, J. Petzelt, I. Gregora, Z. Zikmund, D. Ivannikov, G. Komandin, A. Volkov, and B. Strukov, Phys. Status Solidi B **214**, 423 (1999).
[33] E. Buixaderas, S. Kamba, N. Kolpakova, and J. Petzelt, Eur. Phys. J. **19**, 9 (2001).
[34] E. von Schweidler, Ann. Phys. (Leipzig) **24**, 711 (1907).
[35] H. Fröhlich, *Theory of Dielectrics* (Clarendon Press, Oxford, 1949).
[36] E. Courtens and H. Vogt, Z. Phys. B: Condens. Matter **62**, 143 (1986).
[37] Z.-Y. Cheng, R.S. Katiyar, X. Yao, and A. Guo, Phys. Rev. B **55**, 8165 (1997).
[38] S. Kamba, V. Bovtun, J. Petzelt, I. Rychetský, R. Mizaras, A. Brilingas, J. Banys, J. Grigas, and M. Kosec, J. Phys.: Condens. Matter **12**, 497 (2000).
[39] S. Kamba, V. Porokhonskyy, A. Pashkin, V. Bovtun, J. Petzelt, J. C. Nino, S. Trolier-McKinstry, C. A. Randall, and M. T. Lanagan (to be published).
[40] K.L. Ngai, J. Chem. Phys. **110**, 10 576 (1999), and references therein.
[41] J. Ross Macdonald, J. Chem. Phys. **115**, 6192 (2001).
[42] H.J. Brückner, E. Courtens, and H.-G. Unruh, Z. Phys. B: Condens. Matter **73**, 337 (1988).
[43] P. He, K. Deguchi, M. Hirokane, and E. Nakamura, J. Phys. Soc. Jpn. **59**, 1835 (1990).
[44] J. Petzelt, S. Kamba, A.V. Sinitski, A.G. Pimenov, A.A. Volkov, G.V. Kozlov, and R. Kind, J. Phys.: Condens. Matter **5**, 3573 (1993).
[45] Z. Kutnjak, C. Filipič, A. Levstik, and R. Pirc, Phys. Rev. Lett. **70**, 4015 (1993).
[46] A. Levstik, Z. Kutnjak, C. Filipič, and R. Pirc, Phys. Rev. B **57**, 11 204 (1998).
[47] Z. Kutnjak, C. Filipič, R. Pirc, and A. Levstik, Phys. Rev. B **59**, 294 (1999).
[48] G. Careri, G. Consolini, Z. Kutnjak, C. Filipič, and A. Levstik, Phys. Rev. E **64**, 052901 (2001).